Acoustic of a perforated liner with grazing flow: Floquet-Bloch periodical approach versus impedance continuous approach

Xiwen Dai[a] and Yves Aurégan
Laboratoire d'Acoustique de l'Université du Maine, UMR CNRS 6613, Avenue O Messiaen, F-72085 LE MANS Cedex 9, France

(Received 13 April 2016; revised 4 August 2016; accepted 27 August 2016; published online 27 September 2016)

The effect of a shear flow on an acoustic liner consisting of a perforated plate backed by cavities is studied. Two different approaches are investigated: First, the duct and the liner are considered as a periodic system while in the second approach the liner is considered as homogeneous and described by an impedance. Those two approaches coincide perfectly without flow for a small hole spacing compared to the acoustic wavelength. This work demonstrates that those two approaches are not wholly consistent when a shear flow is present and reveals some problems in the use of the local impedance with flow. The no-flow impedance cannot be used to describe the liner when a shear flow is present. An equivalent impedance with flow can be defined but it depends on the direction of the incident waves and loses its local characteristic. © *2016 Acoustical Society of America*.
[http://dx.doi.org/10.1121/1.4962490]

[JDM] Pages: 2047–2055

I. INTRODUCTION

Acoustic treatments using perforated plates backed by cavities are commonly used to suppress the noise emission from ducts, from air conditioning systems to aircraft engines. In most of these applications, a mean flow is present in the ducts. The acoustic behavior of such treatments in the presence of a grazing flow is a challenging subject due to the complexity of the interaction between sound and flow in the boundary layer and, in particular, near the perforations.

For the locally reacting perforated liner, the acoustic modeling is performed in two steps. The first step consists of substituting the surface of the acoustic treatment by an equivalent impedance. In fact, that means replacing a discrete problem (hole by hole) with a continuous problem. The second step consists in calculation the acoustic propagation in a flow duct with an impedance boundary condition at the walls.

This second step has received significant attention in the past years. A lot of methods have been developed to solve this important practical problem numerically (see, for instance, Ref. 1 and the references therein) either for uniform flow or shear flow. In the recent years, a particular effort has been put on the effect of the boundary layer of the grazing flow on propagation over an impedance surface. In the commonly used model proposed by Myers,[2] the boundary layer is described by a vortex sheet, but the limitations of this model have been revealed recently. Among these limitations, it appears that: It is a not a well-posed problem in the time domain,[3] it is not able to properly predict the instabilities appearing over a liner,[4] it cannot explain the differences between experimentally observed liner effects on the waves propagating in the direction of flow and in the opposite direction to the flow.[5] That is why more and more studies used a shear profile of velocity rather than a uniform profile with Myers condition.[6] The general idea in the study of the Myers or the modified Myers[7] is to let the thickness of the boundary layer (δ^*_{BL} in Fig. 1) tend toward zero. The question that arises here is "why real efforts are made for a fine description in the direction normal to the wall while, at the same time, the longitudinal effects are not taken into account?"

The first step is very often implicit in the previous works. It is generally accepted that a perforated plate backed by cavities can be acoustically described as an impedance when the longitudinal characteristic sizes (D^* and W^* in Fig. 1) are much smaller than the acoustic wavelength. In this case, the only remaining problem is to find this equivalent impedance. An ill-defined part of the flow effect is indeed included in this equivalent impedance while the other part is accounted for in the propagation. A lot of empirical models have been developed to account for the flow effects on the impedance of perforations.[8–14] However, it is difficult to find a model that gives good prediction under different flow and acoustic conditions. Recently, direct numerical simulations (DNSs) or large eddy simulations (LESs) have been used to study the flow effect on liner impedance.[15–18] The DNS and LES models provide a detailed description of the flow-acoustic coupling and give more accurate impedance predictions at the cost of long calculation time. The flow and the acoustic are computed hole by hole, but the final result is again a prediction of an equivalent impedance.

The assumption that a discrete perforated liner with grazing flow can be acoustically described as a continuous impedance has not been previously investigated. This has been demonstrated without flow for one-dimensional cases[19] or for surface waves[20] in the low frequency limit (wavelength much larger than the cell size). This assumption in presence of a mean shear flow will be questioned in the present paper. For that, a very simplified configuration will be

[a]Electronic mail: xiwen.dai@univ-lemans.fr

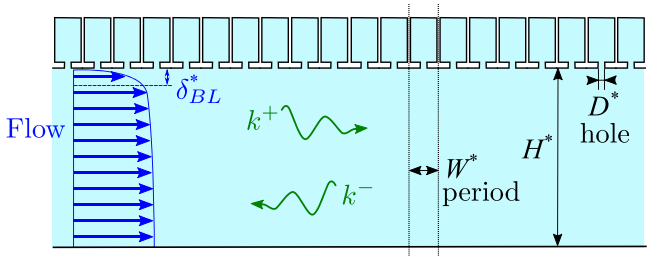

FIG. 1. (Color online) Sketch of an array of periodic cells.

studied. A two-dimensional (2D) array of periodic cells (see Fig. 1) is considered. A shear flow, vanishing on the upper wall, is present which is supposed to be uniform in the longitudinal direction and all the turbulent effects are neglected. The acoustic and hydrodynamic perturbations are linear and lossless and they could be described by the linearized Euler equations (LEEs). In this rather idealized case, the waves that can propagate in this periodic system are determined using the Floquet-Bloch theorem. The wave propagation is split into a 2D periodic field modulated by a plane wave of wavenumber k_B. From the transfer matrix linking some quantities on one side of a cell to the same quantities on the other side, the Bloch wavenumbers k_B can be calculated. If this discrete system can be described with an equivalent impedance, there exists a value Z_{eq} such as the acoustical problem, with the same shear flow and with the upper wall boundary condition $p = Z_{\text{eq}}v$ where p is the acoustic pressure and v is the acoustic normal velocity, will give the same results in terms of wavenumbers that the discrete problem. This equivalent impedance Z_{eq} should depend only on the geometry of the problem and possibly on the mean flow characteristics, but Z_{eq} should not depend on the direction of the incident waves (locally reacting hypothesis). The main finding of this paper is that this equivalent impedance Z_{eq} does not always exist.

In Sec. II A, the multimodal method used to compute the discrete simplified configuration is described. This computation method is applied to fully solve the discrete linearized problem without losses, and to compare later its results to the continuous problem. Then, in Sec. II B, the calculation of the Bloch wavenumbers is detailed while Sec. II C explains how to compute, in the continuous approach, an equivalent impedance Z_{eq} in a shear flow when the wavenumber is known or inversely how to compute the wavenumbers when the impedance is known. The results without flow are discussed in Sec. III A and the results with flow are described in the following Secs. III B–III D, and they show a fundamental problem in the definition of an impedance with a shear flow.

II. NUMERICAL MODEL

A. Computation by multimodal method in a cell with shear flow

In the 2D unit cell shown in Fig. 2(a), the effects of viscosity and the nonlinear effects are neglected and the propagation of small disturbances about a steady mean flow can be described by the LEE

$$\rho_0^*\left(\frac{\partial}{\partial t^*}+U^*\frac{\partial}{\partial x^*}\right)u^*+\rho_0^*\frac{\mathrm{d}U^*}{\mathrm{d}y^*}v^*=-\frac{\partial p^*}{\partial x^*}, \tag{1}$$

$$\rho_0^*\left(\frac{\partial}{\partial t^*}+U^*\frac{\partial}{\partial x^*}\right)v^*=-\frac{\partial p^*}{\partial y^*}, \tag{2}$$

$$\frac{1}{\rho_0^* c_0^{*2}}\left(\frac{\partial}{\partial t^*}+U^*\frac{\partial}{\partial x^*}\right)p^*=-\left(\frac{\partial u^*}{\partial x^*}+\frac{\partial v^*}{\partial y^*}\right), \tag{3}$$

where ρ_0^* is the mean density, c_0^* is speed of sound, and U^*, which is a function of y^* only, is the mean flow velocity, u^* and v^* are the velocity disturbance in, respectively, the x- and y-directions, and p^* is the pressure disturbance. (In this paper, all the quantities with a star are quantities with dimensions while all the quantities without a star are dimensionless quantities.) The quantities are put in dimensionless form by

$$p=\frac{p^*}{\rho_0^* c_0^{*2}},\quad (x,y)=\left(\frac{x^*}{H^*},\frac{y^*}{H^*}\right),\quad (u,v)=\left(\frac{u^*}{c_0^*},\frac{v^*}{c_0^*}\right),$$
$$\omega=\frac{\omega^* H^*}{c_0^*},\quad M(y)=M_0 f(y)=\frac{U^*(y)}{c_0^*},\quad t=\frac{t^* c_0^*}{H^*},$$

where H^* is the height of the duct, ω^* is the angular frequency, and M is the Mach number. M_0 denotes the average Mach number in the duct, with the mean flow profile prescribed by the function $f(y)$. The variables are sought in the form

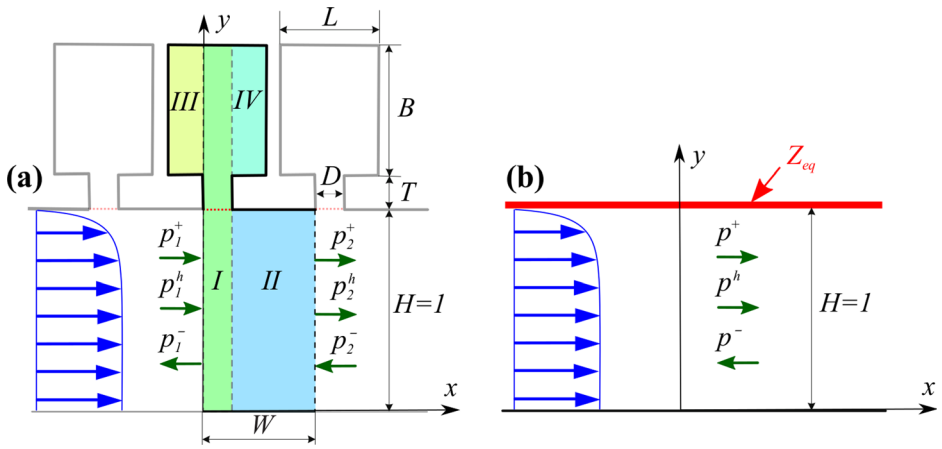

FIG. 2. (Color online) Sketch of (a) one periodic cell and (b) the equivalent continuous system.

$$p = P(y)\exp(-\mathrm{i}kx)\exp(\mathrm{i}\omega t),$$
$$v = V(y)\exp(-\mathrm{i}kx)\exp(\mathrm{i}\omega t),$$
$$q = Q(y)\exp(-\mathrm{i}kx)\exp(\mathrm{i}\omega t), \tag{4}$$

where $\mathrm{i}^2 = -1$, $q = \mathrm{i}\,\partial p/\partial x$, and k is dimensionless wavenumber. Equation (2) is written in term of these new variables as

$$\mathrm{i}(\omega - M_0 fk)V = -\frac{\mathrm{d}P}{\mathrm{d}y}. \tag{5}$$

Removing the axial velocity from Eqs. (1) and (3) leads to

$$\left(1 - M_0^2 f^2\right)k^2 P + 2\omega M_0 fkP - \omega^2 P - \frac{\mathrm{d}^2 P}{\mathrm{d}y^2} = -2\mathrm{i}M_0 \frac{\mathrm{d}f}{\mathrm{d}y} kV. \tag{6}$$

This formulation of the equation is close to the classical Pridmore-Brown equation, which is obtained when the value of V extracted from Eq. (5) is inserted in Eq. (6).

A unit cell of a perforated liner in a flow duct is sketched in Fig. 2(a) and is split into four zones (denoted by roman number). To solve this problem of linear propagation in a shear flow, the multimodal method is used.[21] The mean shear flow is assumed to be unchanged along the flow duct, i.e., the flow profile is the same everywhere when $y < 1$ while the mean flow velocity is 0 in the orifice and inside the cavity, i.e., $y > 1$. In the multimodal analysis, the pressure disturbances in the ducts are expressed as a linear combination of modes, which include acoustic modes and hydrodynamic modes. Equations (5) and (6) are discretized in the y-direction by taking N_1 equally spaced points in zone II, N_2 equally spaced points in zone I, and N_4 equally spaced points in zones III and IV. The spacing between interior points in all segments is $\Delta h = H/N_1 = (H+T+B)/N_2 = B/N_4$, and the first and last points are taken $\Delta h/2$ from the duct walls. The centered finite difference method is used to solve the problem. The following generalized eigenvalue problem coming from Eqs. (5) and (6) and using $kP = Q$ is formed in each of the segments

$$k\begin{pmatrix} \mathbf{I} - M_0^2\mathbf{f}^2 & 2\mathrm{i}M_0\mathbf{f_a} & 0 \\ 0 & \mathrm{i}M_0\mathbf{f} & 0 \\ 0 & 0 & \mathbf{I} \end{pmatrix}\begin{pmatrix} \mathbf{Q} \\ \mathbf{V} \\ \mathbf{P} \end{pmatrix} = \begin{pmatrix} -2\omega M_0\mathbf{f} & 0 & \omega^2\mathbf{I} + \mathbf{D}_2 \\ 0 & \mathrm{i}\omega\mathbf{I} & \mathbf{D}_1 \\ \mathbf{I} & 0 & 0 \end{pmatrix}\begin{pmatrix} \mathbf{Q} \\ \mathbf{V} \\ \mathbf{P} \end{pmatrix}, \tag{7}$$

where $\mathbf{I}$ is the identity matrix, $\mathbf{f}$, $\mathbf{f}_2$, and $\mathbf{f_a}$ are diagonal matrices on the diagonal with the values of f, f^2, and $\mathrm{d}f/\mathrm{d}y$ at the discrete points in the ducts. $\mathbf{Q}$, $\mathbf{V}$, and $\mathbf{P}$ are the column vectors giving, respectively, the value of $Q(y)$, $V(y)$, and $P(y)$ at the discrete points. $\mathbf{D}_1$ and $\mathbf{D}_2$ are matrices for the first and second order differential operator with respect to y. The boundary condition $\mathrm{d}p/\mathrm{d}y = 0$ on the duct walls are taken into account in the differential operator matrices. Solving the eigenvalue problem (7) gives the eigenmodes and the corresponding wavenumbers in the ducts. In zone II, $3N_1$ modes are found, including N_1 acoustic modes propagating or decaying (evanescent modes) in the $+x$ direction, N_1 acoustic modes propagating or decaying in the $-x$ direction, and N_1 hydrodynamic modes propagating in the $+x$ direction. In zone I, the mean flow velocity and its derivative are zero at discrete points where $y > 1$. The last $N_2 - N_1$ rows and columns of the middle parts in the matrices in Eq. (7) and the last $N_2 - N_1$ elements of $\mathbf{V}$ are skipped, corresponding to the no-flow part of this segment. Thus, there are N_2 acoustic modes propagating or decaying both in the $+x$ direction and in the $-x$ direction, and N_1 hydrodynamic modes propagating in the $+x$ direction in zone I. In zones III and IV (no flow), $2N_4$ modes are found: N_4 acoustic modes propagating or decaying in the $+x$ direction, N_4 acoustic modes propagating or decaying in the $-x$ direction.

A resistive layer, as displayed by the dashed lines in Fig. 2(a) for $y = 1$ and $0 < x < D$, is introduced in the orifice. It gives a pressure jump that is proportional to the normal velocity,

$$\Delta p_{y=1} = R v_{y=1} \quad \text{for } 0 < x < D. \tag{8}$$

This resistance R is introduced to mimic the effects of a resistive sheet like a wiremesh or to mimic the hole resistance due to thermo-viscous effects. The introduction of the resistance requires a pressure jump defined in Eq. (8) being taken into account in the formulation. The details of the implementation are given in the Appendix.

The eigenvalues for zones I and II are given in Fig. 3. Two main points can be noted: In zone I, one of the hydrodynamic modes is convectively unstable meaning that an hydrodynamic perturbation created near $x = 0$ can be amplified near $x = D$, the second point is that the hydrodynamic modes in region II, that are naturally neutral, have been artificially damped by multiplying the hydrodynamic wavenumber by $1 - \mathrm{i}e$. This damping has been added to mimic the effect of turbulence that dissipates quickly the coherent hydrodynamic waves in the boundary layer. The used value $e = 0.4$ has been chosen so that the hydrodynamical waves

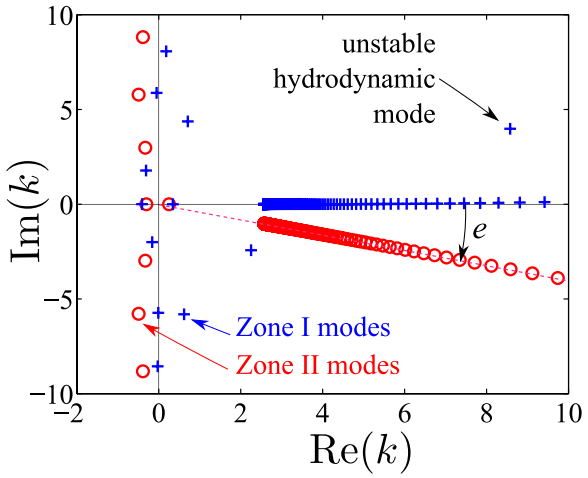

FIG. 3. (Color online) Eigenvalues in zones I and II. The computations are made at a frequency $\omega = 0.274$ with a Mach number $M_0 = 0.1$ and $m = 15$, where m is the parameter determining the shear flow profile [see Eq. (16)].

are completely attenuated in zone II and that no hydrodynamical interactions exist between the holes. It has been shown in Ref. 22 that the hydrodynamic interaction can be neglected when the wall length between successive openings is larger than the opening width.

In each zone, the column vectors giving the values of $P(y)$, $V(y)$, and $Q(y)$ are written as a linear combination of the eigenvectors of the problem [Eq. (7)]

$$\mathbf{P^j}(x) = \sum_{n=1}^{N} C_n^j \mathbf{P_n^j} \exp(-\mathrm{i}k_n^j x),$$

$$\mathbf{V^j}(x) = \sum_{n=1}^{N} C_n^j \mathbf{V_n^j} \exp(-\mathrm{i}k_n^j x),$$

$$\mathbf{Q^j}(x) = \sum_{n=1}^{N} C_n^j \mathbf{Q_n^j} \exp(-\mathrm{i}k_n^j x),$$

where j is the index of the zone (from I to IV), n is the index of the mode, ${}^t(\mathbf{Q_n^j}, \mathbf{V_n^j}, \mathbf{P_n^j})$ is the nth eigenvector of Eq. (7) in the zone j, C_n^j is the coefficient of the nth mode in zone j. $N = 3N_1$ in zone II, $N = N_1 + 2N_2$ in zone I, and $N = 2N_4$ in zones III and IV.

Once the modes are found in each duct segment, they are matched between each zone [see Fig. 2(a)]. At the interfaces between zones I and II, the continuity of p, v, and q is applied. At the interfaces between zones I, III, and IV, the continuity of p and q is applied. On the vertical solid walls, the x-direction velocity vanishes and so $q = 0$. These continuity conditions can be put in the form of a large matrix that links all the incoming waves in the cell to outgoing waves and to all the internal variables. From this large matrix, the scattering matrix is written

$$\begin{pmatrix} \mathbf{C_2^+} \\ \mathbf{C_1^-} \end{pmatrix} = \mathsf{S} \begin{pmatrix} \mathbf{C_1^+} \\ \mathbf{C_2^-} \end{pmatrix}, \tag{9}$$

where vectors C_1^+ (respectively, C_2^+) contain the duct mode coefficients for $x = 0$ (respectively, $x = W$) for a wave going in the flow direction (respectively, for wave propagation opposite to the flow) and

$$\mathsf{S} = \begin{pmatrix} \mathsf{T}^+ & \mathsf{R}^- \\ \mathsf{R}^+ & \mathsf{T}^- \end{pmatrix},$$

where T^+ $(2N_1 \times 2N_1)$, R^+ $(N_1 \times 2N_1)$, T^- $(N_1 \times N_1)$, and R^- $(2N_1 \times N_1)$ are transmission and reflection matrices with and against the mean flow. The matrices have different sizes because N_1 acoustic and N_1 hydrodynamic modes propagate in the $+x$-direction while N_1 acoustic modes propagate in the $-x$-direction in zone II.

B. Computation of wavenumbers using the Floquet-Bloch theorem

When the governing equations, the boundary conditions, and the geometry are W-periodic along x, the Floquet-Bloch theorem states that the solution of any quantities ϕ can be written[23–25]

$$\phi(x, y) = \hat{\phi}(x, y) e^{-\mathrm{i}k_B x}, \tag{10}$$

i.e., the function $\phi(x, y)$ can be split into a W-periodic field $\hat{\phi}(x, y)$ modulated by a plane wave with the Bloch wavenumber k_B. This decomposition into a periodic part modulated by an exponential term is as general for periodic systems as the mode concept for a homogeneous system. This relation leads to $\phi(W, y) = \mathrm{e}^{-\mathrm{i}k_B W}\phi(0, y)$, which can be written in vectorial form for the unit cell

$$\begin{pmatrix} \mathbf{C_2^+} \\ \mathbf{C_2^-} \end{pmatrix} = \mathrm{e}^{-\mathrm{i}k_B W} \begin{pmatrix} \mathbf{C_1^+} \\ \mathbf{C_1^-} \end{pmatrix}. \tag{11}$$

The scattering relation of the modal waves in Eq. (9) can be rewritten as

$$\mathsf{M}_1 \begin{pmatrix} \mathbf{C_1^+} \\ \mathbf{C_1^-} \end{pmatrix} = \mathsf{M}_2 \begin{pmatrix} \mathbf{C_2^+} \\ \mathbf{C_2^-} \end{pmatrix}, \tag{12}$$

where

$$\mathsf{M}_1 = \begin{pmatrix} \mathsf{T}^+ & 0 \\ -\mathsf{R}^+ & \mathsf{I} \end{pmatrix}, \quad \mathsf{M}_2 = \begin{pmatrix} \mathsf{I} & -\mathsf{R}^- \\ 0 & \mathsf{T}^- \end{pmatrix}.$$

Equations (11) and (12) lead to a generalized transfer matrix eigenvalue problem of a unit cell of the liner,

$$\mathsf{M}_1 \begin{pmatrix} \mathbf{C_1^+} \\ \mathbf{C_1^-} \end{pmatrix} = \mathrm{e}^{-\mathrm{i}k_B W} \mathsf{M}_2 \begin{pmatrix} \mathbf{C_1^+} \\ \mathbf{C_1^-} \end{pmatrix}. \tag{13}$$

Solving the eigenvalue problem in Eq. (13) gives the Floquet-Bloch wavenumbers.

C. Method for solving the continuous problem

In the case where the cell is substituted by an equivalent impedance, see Fig. 2(b), the propagation is described by the same LEEs (5) and (6) but the boundary condition at the wall $y = 1$, where the mean velocity vanishes, is $P(1) = Z_{\mathrm{eq}} V(1)$. To solve this problem when the wavenumber k is known, the new variable Y such as $\mathrm{d}P/\mathrm{d}y = YP$ is introduced. The variation of Y is given by

$$\frac{\mathrm{d}Y}{\mathrm{d}y} = -Y^2 - \frac{2M_0 k}{\omega - M_0 f k} \frac{\mathrm{d}f}{\mathrm{d}y} Y - (\omega - M_0 k f)^2 + k^2. \tag{14}$$

This equation can be integrated by means of the fourth-order Runge-Kutta scheme from the lower hard wall ($y = 0$) where $Y(0) = 0$ to the upper impedance wall ($y = 1$). The equivalent liner impedance is obtained from $Z_{\mathrm{eq}} = -\mathrm{i}\omega/Y(1)$. On the other hand, if an impedance is prescribed at the wall, the eigenvalue problem (7), with modifications in the matrices $\mathbf{D}_1$ and $\mathbf{D}_2$ to take into account the impedance condition, can be used to find the wavenumbers. It is noted that the resolution of the Eq. (14) can be difficult when $\omega - M_0 f(y) k$ is zero or close to zero. But, here we are looking for the acoustical mode for which k is imposed and is not embedded in

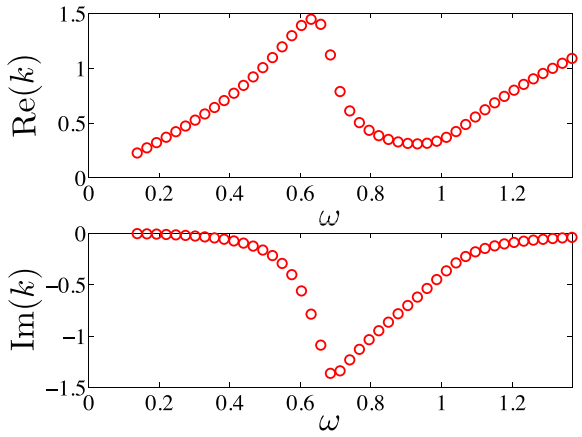

FIG. 4. (Color online) Real and imaginary parts of the Bloch wavenumber k_{B0}^{+} of the least attenuated mode in the $+x$-direction.

the continuum of hydrodynamic modes. Thus, we have not observed numerical difficulties when integrating Eq. (14).

III. RESULTS

Calculations in the following are carried out on a 2D perforated liner having dimensions of the same order as those used in aircraft engines. The perforated plate has a thickness $T^* = 0.5$ mm with an orifice size $D^* = 1$ mm and a percentage of open area (POA) $\sigma = D^*/W^* = 20\%$ ($W^* = 5$ mm). The cavities have a depth of $B^* = 25$ mm. The POA of the backing cavities is supposed to be 100% ($L^* = W^* = 5$ mm). The first resonant frequency of this liner is 2729 Hz (see Sec. III A) and the calculations are made for frequencies between 500 and 5000 Hz. At the entrance of the perforation a thin layer with a normalized resistance $R = 0.05$ has been added.

The height of the duct is equal to $H^* = 15$ mm to have values comparable to Ref. 5. In this case, the cut-on frequency for the first non-plane mode is equal to $c_0/(2H) = 11\,500$ Hz in a rigid duct. Thus, for the frequency range under study, only one mode propagates in each direction without flow. To see the effect of the liner on higher propagative modes, some calculations have been performed for $H^* = 100$ mm where the cut-on frequencies for the first rigid modes are 1720, 3440, and 5160 Hz.

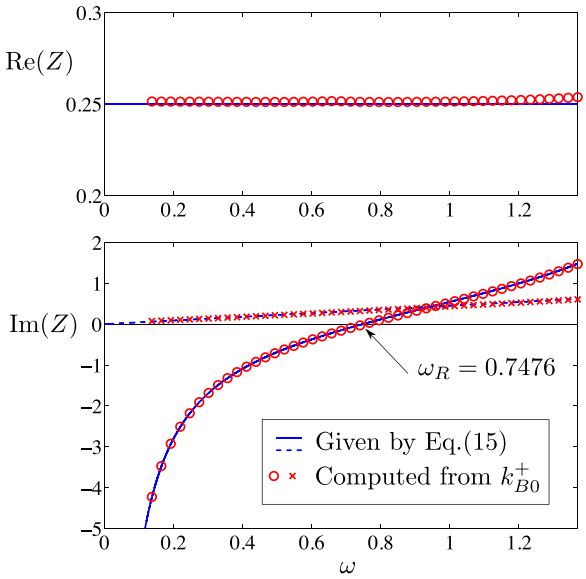

FIG. 5. (Color online) Comparison between the impedance computed using the less attenuated Bloch mode (symbols) and Eq. (15) (lines). The circles and the continuous lines represent the liner impedance Z_0 while the crosses and the dashed line represent the perforated plate impedance by removing the effect of the cavity $Z_p = Z_0 + \mathrm{i}/\tan(\omega B)$. The Bloch wavenumbers have been computed without flow.

A. Case without flow

To test our approach, the case without flow is considered. First, the Bloch wavenumbers are computed without flow. In the no-flow case, the Bloch wavenumbers are opposite two by two and the wavenumber k_{B0}^{+} of the least attenuated mode in the $+x$-direction is displayed in Fig. 4. Then, the equivalent impedance is computed by integrating Eq. (14) and the result is given in Fig. 5. The equivalent impedance is in good accordance to the theoretical value given by

$$Z_0 = \frac{1}{\sigma}(R + \mathrm{i}\omega(T + \delta_T)) - \frac{\mathrm{i}}{\tan(\omega B)}, \tag{15}$$

where $\sigma = D^*/W^*$ is the POA and $\delta_T^* = 0.85$ mm is the added length of the hole, which has been empirically determined from the calculation.

Figure 6 shows the comparison of the wavenumbers computed by the continuous model using the equivalent impedance Eq. (15) and the Bloch wavenumbers. The good

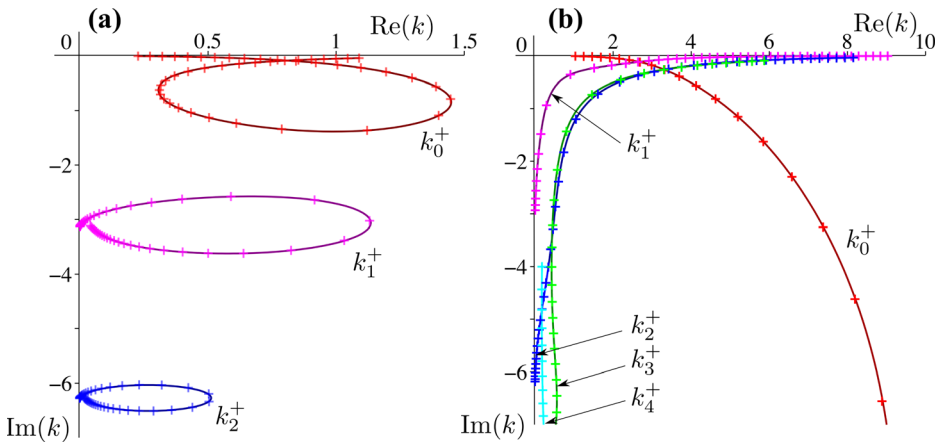

FIG. 6. (Color online) Comparison without flow of the wavenumbers for a frequency sweep from $\omega = 0.137$ to $\omega = 1.37$, computed by the continuous model using the equivalent impedance Eq. (15) (lines) and the Bloch wavenumbers (symbols). (a) $H^* = 15$ mm, (b) $H^* = 100$ mm.

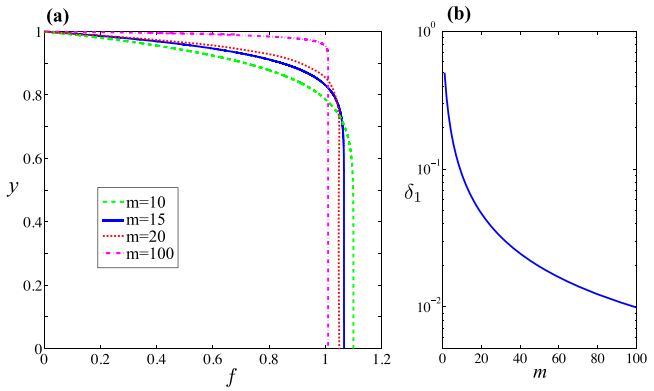

FIG. 7. (Color online) (a) The mean flow profile for different values of the parameter m. (b) Displacement boundary layer thickness as a function of the parameter m.

accordance between the wavenumbers of the continuous model and the Bloch wavenumbers has also been verified for the higher attenuated modes and in the case of a larger duct ($H^* = 100$ mm) where several modes can propagate.

The wavenumbers computed from the discrete model and the wavenumbers computed from an equivalent impedance are the same without flow. Thus, the discrete system can be accurately described, even for highly attenuated modes, by a continuous model without flow in the regime where the wavelength is large compared to the cell length.

B. Convergence of the solutions with flow

To compute solutions with shear flow, a simple polynomial law with a unity average value had been chosen

$$f = f_0(1 - y^m) \quad \text{with } f_0 = \frac{m+1}{m}, \tag{16}$$

where the parameter m can be varied to change the thickness of the boundary layer. The mean flow profiles are plotted in Fig. 7(a) and the variation of the displacement thickness $\delta_1 = \int_0^1 (1 - f/f_0)\mathrm{d}y = 1/(m+1)$ is plotted in Fig. 7(b) as a function of m.

As an example, the Bloch wavenumbers are computed with a flow profile given by $m = 15$ and at a frequency $\omega = 2\pi f^* H^*/c_0^* = 0.274$ (corresponding to 1000 Hz). The number of points N_1 is varied and the result is compared to a reference result computed with $N_{1R} = 1920$. The estimated error $\Delta = |k_B(N_1) - k_B(N_{1R})|/|k_B(N_{1R})|$ is plotted as a function of the number of points in Fig. 8(a). It can be seen in Fig. 8 that the computation converges as N_1^{-3}. Thus, the resulting impedance Z_{eq} converges also as indicated in Figs. 8(b) and 8(c) where two values of the plate impedance $Z_p = Z_{\mathrm{eq}} + \mathrm{i}/\tan(\omega B)$, resulting from the least attenuated modes in the $+x$-direction (k_{B0}^+) and in the $-x$-direction (k_{B0}^-) are plotted.

In Figs. 8(b) and 8(c), one of the main results of this paper can be seen: With flow, the equivalent impedance describing the continuous system that can be computed from the Bloch wavenumbers differs from the impedance without flow and differs when the propagation direction is modified. The fact that the equivalent impedance converges to two different values, when the propagation direction is reversed, is clearly incompatible with the continuous model that calculates the entire propagation from a single impedance value.

C. Case with flow

To confirm the above conclusions, the Bloch wavenumbers for the two least attenuated modes are plotted as a function of frequency on Fig. 9 for a shear flow with $M_0 = 0.3$ and $m = 15$. Figure 9 displays also the wavenumbers computed from the continuous model with the impedance without flow given by Eq. (15). It can be clearly seen that a continuous model using the no-flow impedance cannot be used to describe the propagation in the discrete system.

The two impedances deduced from k_{B0}^+ and k_{B0}^- by integrating Eq. (14) with the same shear flow are plotted in Fig. 10. To see more clearly the flow effects, the impedance of the backing cavity have been removed from the imaginary part. These two impedances differ from one another and are different from the no-flow impedance.

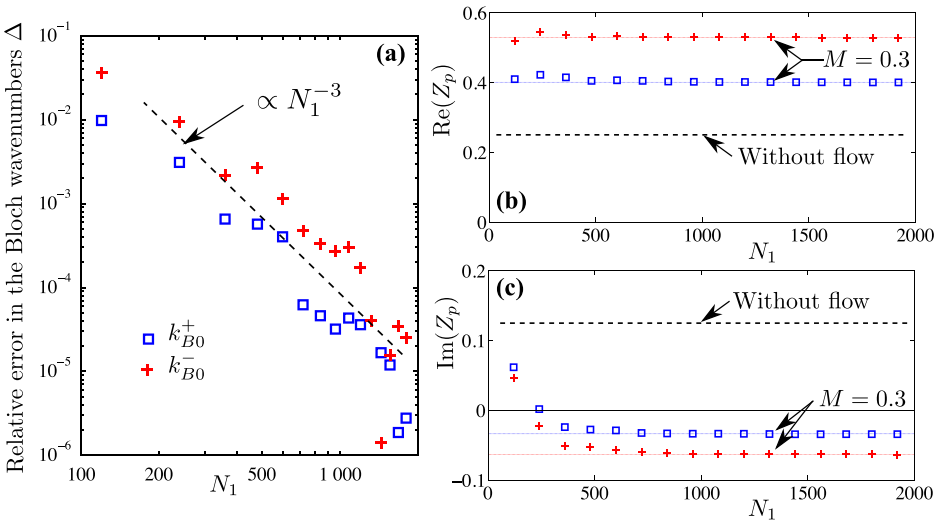

FIG. 8. (Color online) (a) Relative error in the Bloch wavenumbers Δ as a function of the number of points N_1. Value of (b) the real part and (c) the imaginary part of the plate impedance Z_p as a function of N_1. The square symbols indicate the values of impedance computed from the least attenuated Bloch wavenumber propagating in the flow direction k_{B0}^+, and the plus symbols refer to the least attenuated Bloch wavenumber propagating in the direction opposite to the flow k_{B0}^-. The computations are made at a frequency $\omega = 0.274$ with a Mach number $M_0 = 0.3$ and $m = 15$.

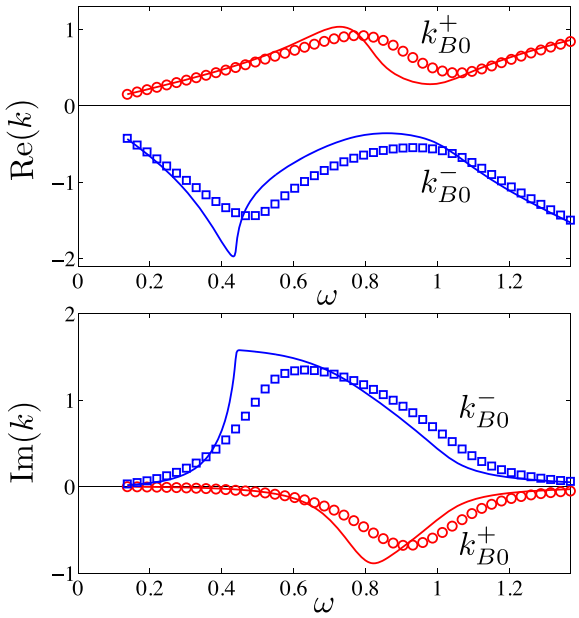

FIG. 9. (Color online) Real and imaginary parts of wavenumbers for the two least attenuated the Bloch waves. The circle symbols indicate the values of the least attenuated Bloch wavenumber propagating in the flow direction k_{B0}^{+} and the square symbols are the least attenuated Bloch wavenumber propagating in the direction opposite to the flow k_{B0}^{-}. The lines represent the wavenumbers in the continuous model computed using the no-flow impedance. The computations are made with a Mach number $M_0 = 0.3$ and $m = 15$.

It means that two different equivalent impedances are required in the continuous system to depict the propagations of k_{B0}^{+} and k_{B0}^{-} modes. In other words, it is impossible to find a value of the impedance that can fully describe the effect of the periodic array of resonators on sound propagation in a shear flow.

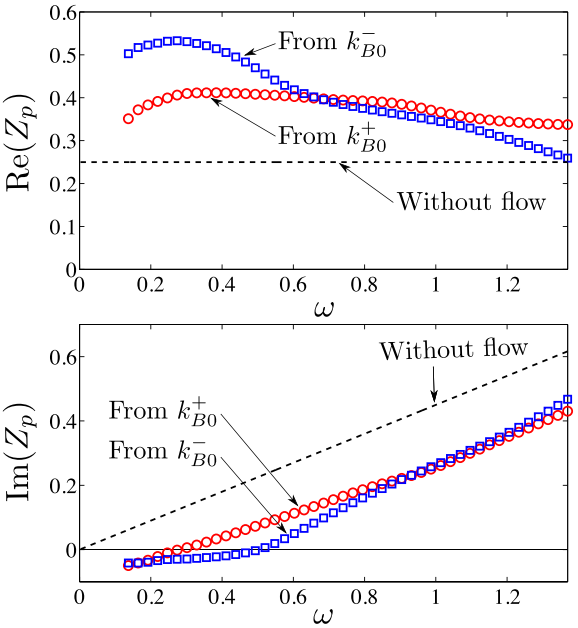

FIG. 10. (Color online) Real and imaginary parts of the equivalent plate impedance as a function of the frequency. The circle symbols indicate the values of impedance computed from the least attenuated Bloch wavenumber propagating in the flow direction k_{B0}^{+} and the square symbols refer to the least attenuated Bloch wavenumber propagating in the direction opposite to the flow k_{B0}^{-}. The computations are made with a Mach number $M_0 = 0.3$ and $m = 15$.

D. Influence of flow velocity and boundary layer thickness on liner impedance

The influence of the mean Mach number and the boundary layer thickness on liner impedance can be observed in Figs. 11 and 12. Generally, the flow increases the liner resistance and decreases liner reactance. It is shown in Fig. 11 that the resistance increases slowly from the no-flow value at low Mach numbers. When $M_0 > 0.2$, the resistance increases almost linearly with M_0. This trend is consistent with many previous experimental investigations. The present calculations are compared in Fig. 11 with the classical Guess model[10] which says that the normalized impedance of the perforated plate with flow is $Z_p = (R + R_f)/\sigma + \mathrm{i}\omega(T + \delta_f)$ where, for a low sound pressure level: $R_f = 0.3(1 - \sigma^2)M_0$ and $\delta_f = \delta_T x_f$ with $x_f = (1 + 305M_0^3)^{-1}$. It can be seen that the general trend is respected even if the exact values are not recovered by the empirical model. It means that the oversimplified model used in this paper captures some of the flow-acoustic couplings near the liner. The main idea advocated by this comparison is that the equivalent impedance, extracted from shear flow computations, is a quantity that changes when the flow is modified. This is confirmed by the variation of the impedance when the boundary layer thickness varies (see Fig. 12). The variation of the resistance is almost proportional to m (i.e., quasi-inversely proportional to the boundary layer thickness) for $\omega = 0.274$. The hypothesis that the impedance can be kept constant while the boundary layer thickness decreases, which is used for

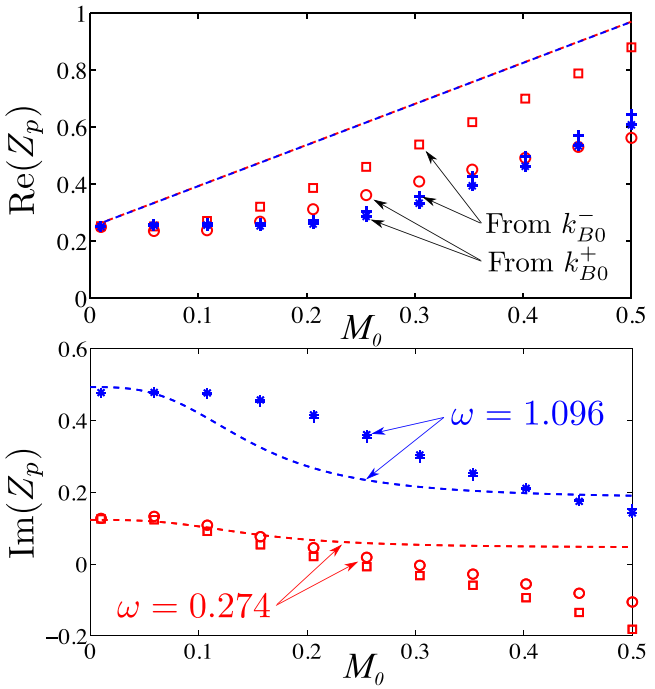

FIG. 11. (Color online) Real and imaginary parts of the equivalent plate impedance as a function of the Mach number. The circle symbols ($\omega = 0.274$) and the cross symbols ($\omega = 1.096$) indicate the values of impedance computed from the least attenuated Bloch wavenumber propagating in the flow direction k_{B0}^{+} and the square symbols ($\omega = 0.274$), and the star symbols ($\omega = 1.096$) refer to the least attenuated Bloch wavenumber propagating in the direction opposite to the flow k_{B0}^{-}. The dashed lines represent the Guess model (Ref. 10). The computations are made with $m = 15$.

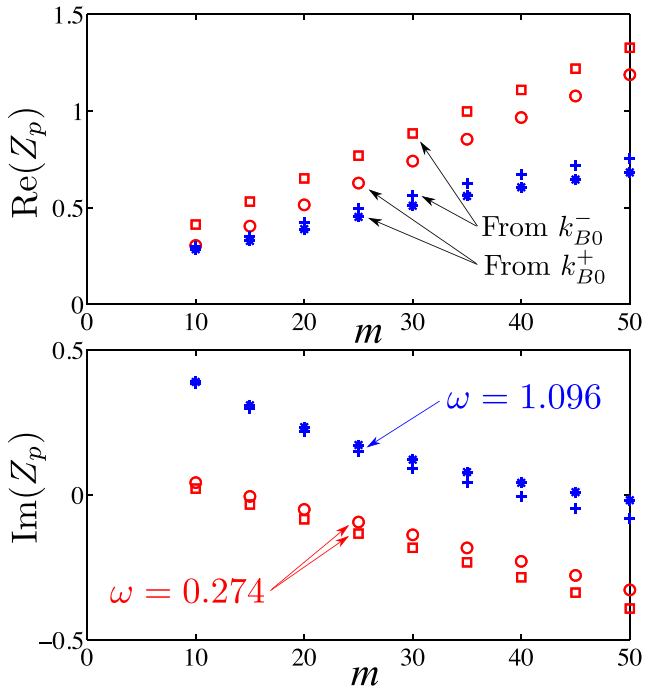

FIG. 12. (Color online) Real and imaginary parts of the equivalent plate impedance as a function of the parameter m controlling the boundary layer thickness. See the caption for Fig. 11. $M_0 = 0.3$.

deriving the Ingard-Myers condition, is questionable (see, for instance, see Ref. 26).

The influence of the flow and acoustic conditions on the difference between the impedances calculated from k_{B0}^+ and k_{B0}^- can be observed in Figs. 10–12. First, the discrepancy shows apparent frequency dependence (see Figs. 10 and 11). Second, it increases with the increasing flow Mach number. For $\omega = 0.274$ and $M_0 = 0.5$, the error in the real part of the impedance can reach one-third of its value. The difference is also affected by the boundary layer thickness, it tends to be more significant in the case with a thinner boundary layer.

IV. CONCLUSION

The effect of a shear flow on an acoustic liner consisting of a perforated plate backed by cavities has been studied. The configuration is typical of some application in the sense that the holes size and the spacing between holes are on the order of the flow boundary layer thickness. Nevertheless, several important effects have not been taken into account in the present calculations like viscosity, turbulence, and nonlinear effects.

Two different approaches have been investigated. The first one considers the duct and the liner as a periodic system, and an exact calculation is performed under the assumptions made in the model. The second approach is used in the vast majority of papers examining acoustic liners. It consists in considering the liner as homogeneous in the axial direction and described by an impedance. It has been shown that those two approaches coincide perfectly without flow when the parameter: hole spacing over acoustic wavelength is small ($\varepsilon_1 = W/\lambda \ll 1$). This work demonstrates that those two approaches are not wholly consistent when a shear flow is present and reveals some problems in the commonly used approach.

First, the no-flow impedance cannot be used to describe the liner with flow. It means that a part of the flow effect that depends on the mean flow value and the boundary layer thickness has to be included into an equivalent corrected impedance that is not well defined. Even more fundamentally, it has been shown that this equivalent impedance depends on the direction of the incident waves. This has already been highlighted experimentally.[5] but it was attributed to a non-complete description of the propagation in a shear flow. In this work, it is demonstrated that the dependence of impedance on the direction of incident waves is due to a more fundamental issue because the propagation in the shear flow is, here, completely described.

This work shows that a modeling effort still needs to be done on the description of liners with flow. The presence of the hydrodynamic modes, the wavelength of which can be small compared to the periodicity, is one of the potential issues in the homogenization process of finding a local impedance. In particular, the classical approach used in the derivation of the Ingard-Myers boundary condition is: First, it is assumed that the wall is homogeneous ($\varepsilon_1 \to 0$) and then the effect of a second small parameter: boundary layer thickness over acoustic wavelength ($\varepsilon_2 = \delta/\lambda$) is studied. This approach appears to be not valid when the two small parameters ε_1 and ε_2 are of the same order.

ACKNOWLEDGMENTS

This work was supported by the French Agence Nationale de la Recherche international project FlowMatAc No. ANR-15-CE22-0016-01.

APPENDIX: INTRODUCTION OF THE RESISTIVE LAYER

In the multimodal analysis, Eq. (8) is equivalent to the following modal relation:

$$\Delta P_{y=1} = R V_{y=1} \quad \text{for } 0 < x < D, \tag{A1}$$

where P and V are modal pressure and velocity, respectively. Employing a second-order expansion of P at $y = 1$ and considering Eqs. (A1) and (5) with the fact that the mean flow velocity is zero at $y = 1$, the pressure jump can be expressed as

$$\Delta P = \frac{-R}{i\omega\Delta h + R}(P_{N_1+1} - P_{N_1}), \tag{A2}$$

where P_{N_1} and P_{N_1+1} are the modal pressure at the N_1th and $(N_1 + 1)$th discrete points.

As a pressure jump is prescribed in Eq. (A1), the discrete derivatives of P with respect to y need to be modified when the centered finite difference scheme involves the discrete points on both sides of the jump. Since the pressure

jump is introduced at $y=1$, i.e., the middle between the N_1th and (N_1+1)th discrete points, the discrete derivatives at these two points need modifications

$$
\begin{aligned}
D_1(P_{N_1}) &= \frac{(P_{N_1+1}+\Delta P)-P_{N_1-1}}{2\Delta h},\\
D_1(P_{N_1+1}) &= \frac{(P_{N_1+2}+\Delta P)-P_{N_1}}{2\Delta h},\\
D_2(P_{N_1}) &= \frac{(P_{N_1+1}+\Delta P)-2P_{N_1}+P_{N_1-1}}{(\Delta h)^2},\\
D_2(P_{N_1+1}) &= \frac{(P_{N_1+2}+\Delta P)-2(P_{N_1+1}+\Delta P)+P_{N_1}}{(\Delta h)^2},
\end{aligned}
\tag{A3}
$$

where D_1 and D_2 denote the first and second discrete derivatives. Submitting Eq. (A2) into Eq. (A3), the amendment in the differential operators $\mathbf{D}_1$ and $\mathbf{D}_2$ in Eq. (7) can be obtained, which takes into account the introduced resistive layer.

[1]R. J. Astley, R. Sugimoto, and P. Mustafi, "Computational aero-acoustics for fan duct propagation and radiation. Current status and application to turbofan liner optimisation," J. Sound Vib. **330**(16), 3832–3845 (2011).
[2]M. K. Myers, "On the acoustic boundary condition in the presence of flow," J. Sound Vib. **71**(3), 429–434 (1980).
[3]E. J. Brambley, "Fundamental problems with the model of uniform flow over acoustic linings," J. Sound Vib. **322**(4), 1026–1037 (2009).
[4]D. Marx and Y. Aurégan, "Effect of turbulent eddy viscosity on the unstable surface mode above an acoustic liner," J. Sound Vib. **332**(15), 3803–3820 (2013).
[5]Y. Renou and Y. Aurégan, "Failure of the Ingard-Myers boundary condition for a lined duct: An experimental investigation," J. Acoust. Soc. Am. **130**(1), 52–60 (2011).
[6]X. Jing, S. Peng, L. Wang, and X. Sun, "Investigation of straightforward impedance eduction in the presence of shear flow," J. Sound Vib. **335**, 89–104 (2015).
[7]E. J. Brambley, "Well-posed boundary condition for acoustic liners in straight ducts with flow," AIAA J. **49**(6), 1272–1282 (2011).
[8]E. J. Rice, "A model for the acoustic impedance of a perforated plate liner with multiple frequency excitation," NASA Technical Report TM-67950, 1971.
[9]D. Ronneberger, "The acoustical impedance of holes in the wall of flow ducts," J. Sound Vib. **24**, 133–150 (1972).
[10]A. W. Guess, "Calculation of perforated plate liner parameters from specified acoustic resistance and reactance," J. Sound Vib. **40**(1), 119–137 (1975).
[11]A. S. Hersh and T. Rogers, "Fluid mechanical model of the acoustic impedance of small orifices," NASA Technical Report CR-2682, 1976.
[12]J. W. Kooi and S. L. Sarin, "An experimental study of the acoustic impedance of Helmholtz resonator arrays under a turbulent boundary layer," AIAA Paper 1981-1998, 1981.
[13]A. Cummings, "The effect of grazing turbulent pipe flow on the impedance of an orifice," Acustica **61**, 233–242 (1986).
[14]T. Elnady and H. Boden, "On semi-empirical liner impedance modeling with grazing flow," AIAA Paper 2003-3304, 2003.
[15]C. K. W. Tam, H. Ju, and B. E. Walker, "Numerical simulation of a slit resonator in a grazing flow under acoustic excitation," J. Sound Vib. **313**(3), 449–471 (2008).
[16]C. K. W. Tam, N. N. Pastouchenko, M. G. Jones, and W. R. Watson, "Experimental validation of numerical simulations for an acoustic liner in grazing flow: Self-noise and added drag," J. Sound Vib. **333**(13), 2831–2854 (2014).
[17]Q. Zhang and D. J. Bodony, "Numerical simulation of two-dimensional acoustic liners with high-speed grazing flow," AIAA J. **49**(2), 365–382 (2011).
[18]Q. Zhang and D. J. Bodony, "Numerical investigation of a honeycomb liner grazed by laminar and turbulent boundary layers," J. Fluid Mech. **792**, 936–980 (2016).
[19]N. Sugimoto and T. Horioka, "Dispersion characteristics of sound waves in a tunnel with an array of Helmholtz resonators," J. Acoust. Soc. Am. **97**(3), 1446–1459 (1995).
[20]L. Kelders, J. F. Allard, and W. Lauriks, "Ultrasonic surface waves above rectangular-groove gratings," J. Acoust. Soc. Am. **103**(5), 2730–2733 (1998).
[21]G. Kooijman, P. Testud, Y. Aurégan, and A. Hirschberg, "Multimodal method for scattering of sound at a sudden area expansion in a duct with subsonic flow," J. Sound Vib. **310**(4), 902–922 (2008).
[22]M. M. G. Derks and A. Hirschberg, "Self-sustained oscillation of the flow along Helmholtz resonators in a tandem configuration," in *8th International Conference on Flow Induced Vibration (FIV)* (2004).
[23]C. E. Bradley, "Time harmonic acoustic Bloch wave propagation in periodic waveguides. Part I. theory," J. Acoust. Soc. Am. **96**(3), 1844–1853 (1994).
[24]B. Nennig, Y. Renou, J. P. Groby, and Y. Aurégan, "A mode matching approach for modeling two dimensional porous grating with infinitely rigid or soft inclusions," J. Acoust. Soc. Am. **131**(5), 3841–3852 (2012).
[25]S. Lidoine, I. Terrasse, T. Abboud, and A. Bennani, "Numerical prediction of SDOF-perforated plate acoustic treatment impedance. Part 1: Linear domain," AIAA Paper 2007-3717, 2007.
[26]Y. Aurégan, R. Starobinski, and V. Pagneux, "Influence of grazing flow and dissipation effects on the acoustic boundary conditions at a lined wall," J. Acoust. Soc. Am. **109**(1), 59–64 (2001).